

STUDY OF COPPER (II) ION ADSORPTION ON SILICA NANOPARTICLE MATERIAL SYNTHESIZED FROM RICE HUSK ASH

Dến tòa soạn: 21-05-2025

Thanh Le Dang Thi* and Thu-Huong Le

(1) Faculty Chemistry and Environment, Thuyloi University, Ha Noi, Viet Nam

*Email: ledtt@tlu.edu.vn

TÓM TẮT

NGHIÊN CỨU HẤP THỤ ION ĐỒNG (II) BẰNG VẬT LIỆU NANO SILICA TỔNG HỢP TỪ TRO TRÁU

Các hạt nano silica tổng hợp từ tro trâu được đánh giá là chất hấp phụ để loại bỏ ion Cu^{2+} khỏi dung dịch nước. Đặc trưng tính chất của nano SiO_2 được xác định bằng các phương pháp SEM, EDX, XRD và BET. Nano SiO_2 chủ yếu là vô định hình, với kích thước hạt khoảng 100 nm và diện tích bề mặt riêng khoảng 250 m^2/gam . Chúng tôi nghiên cứu khả năng của nano SiO_2 trong việc loại bỏ ion Cu^{2+} khỏi dung dịch nước và đánh giá tác động của thời gian, nồng độ hấp phụ và độ pH. Nano SiO_2 tổng hợp từ tro trâu có khả năng hấp phụ hiệu quả ion Cu^{2+} từ dung dịch nước có pH 5-6. Đường đanding nhiệt hấp phụ phù hợp mô hình Langmuir, khả năng hấp phụ tối đa đối với Cu^{2+} là 76,90 mg/g.

Từ khóa: nano silica (nano SiO_2), đường đanding nhiệt hấp phụ, mô hình Langmuir, mô hình Freundlich

1. INTRODUCTION

Clean and safe water is one of the most essential commodities for sustaining life processes. Water contamination with heavy metals such as copper, chromium, cadmium, arsenic, nickel, lead, and mercury is of significant concern due to its hazardous environmental effects [1]. These metals are toxic and are not biodegradable. Moreover, they can infiltrate the food chain, gradually accumulating in living organisms and leading to long-term harmful effects. Today, the strong development of many industries in Vietnam, such as chemicals, paper industry, metallurgy, and electroplating, has made the water environment more and more polluted with heavy metals. In particular, heavy metal pollution in traditional craft villages of Vietnam has became worrying due to the absence of waste collection and treatment

systems. Available methods for heavy metal removal included ion exchange [2], nano-filtration [3], solvent extraction [4], chemical precipitation [5], and adsorptions [6, 7]. Among them, adsorption technology was the most commonly used due to its simplicity, effectiveness, and affordability. Thus, the demand for materials for adsorption of heavy metals in wastewater at low cost has been increasingly urgent. Silica nanoparticle (SiO_2 NP) is an important inorganic material because of its small particle size, large surface area, high chemical purity, and good dispersing properties. Therefore, silica nanoparticles (SiO_2 NPs) have applications in many areas, such as rubber, plastic, ceramics, biomedical, and optics. Recently, super-smooth silica materials have been increasingly studied for applications such as adsorbents: gas adsorption [8], heavy metal ion adsorption [9, 10], and organic

matter adsorption [11]. However, most reported silica synthesis came from expensive TEOS sources [12], limiting the scalability of silica-based materials. Thus, finding available, inexpensive, and silica-rich materials to make this material became interesting. A promising source of material was rice husk ash, one of the richest silica materials, about 90% in volume. Therefore, our group synthesized SiO_2 NPs from rice husk ash and evaluated them as Cu^{2+} adsorbents from aqueous solutions. The structure of as-synthesized SiO_2 NPs samples was characterized by nitrogen adsorption-desorption analyses, X-ray powder diffraction, and scanning electron microscopy with energy dispersive X-ray spectroscopy. The adsorption ability of SiO_2 NPs for removing Cu^{2+} ions from aqueous solution was investigated by evaluating the influence of time, adsorbed dose, and pH on its absorption capacity.

2. EXPERIMENTAL

Chemicals and Characterizations

All chemical reagents, including manganese hydrochloric acid (HCl 36%, $d = 1.18 \text{ g/l}$), sulfuric acid (H_2SO_4), ammonia solution (NH_3 , 25%), sodium hydroxide (NaOH), sodium sulfate (Na_2SO_4), copper sulfate (CuSO_4), and ferric sulfate ($\text{Fe}_2(\text{SO}_4)_3$) were purchased from Shanghai Chemical Reagent Company of China. Nitroso-R salt was purchased from Sigma-Aldrich. In our experiment, the rice husk ash (RHA) was obtained from Me village, Bac Giang province.

X-ray diffraction (XRD) spectra were obtained using D8 Advance (Bruker-Germany) and D5005 (Siemens-Germany). The scanning electron microscopy and energy dispersive X-ray spectroscopy (EDX) measurements were

performed with an S-4800 microscope (SEM, Hitachi). Nitrogen (N_2) adsorption-desorption isotherms were measured at 77K by Quanta chrome Nova Win (USA). The specific surface area of the sample was determined using the Brunauer - Emmett - Teller (BET) method. UV-DR3900 spectrometer (Hach Co., Ltd., USA) was used to obtain the UV-vis absorption spectrum of Cu^{2+} solution in water.

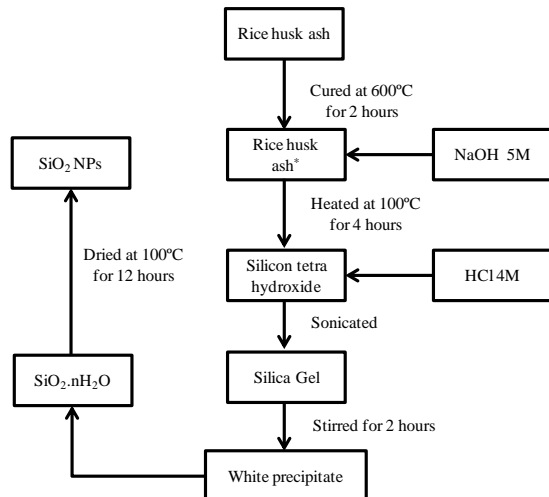
Synthesis of silica nanoparticles (SiO_2 NPs)

Scheme 1 described the synthesis process of SiO_2 NPs from rice hush ask (RHA)

Treatment of RHA

First, RHA was ground and sifted through a sieve of 0.1 mm to obtain a smooth powder. Second, RHA powder was cured in the furnace at 600°C for 2 hours to remove carbon and residual organic substances.

Synthesis of SiO_2 NPs



Scheme 1: Synthesis process of SiO_2 NPs

Based on the work of Zhu *et al.* [9], the synthesis method was improved to be more scalable to industrial scale. We used sonication heating instead of microwave heating and eliminated the addition of

surfactant. Here, 100 g of RHA was stirred with 1000 mL of NaOH 4M at 100°C for 4 hours; the mixture was filtered to obtain a transparent solution. Next, HCl 4M was added to this solution under sonication for 2 hours to reach pH 4. White precipitation appeared. This precipitate was filtered, washed with distilled water, and dried at 100°C in the oven for 12 hours. The final product was a white powder of SiO₂ NPs.

Adsorption experiments

Several factors that could impact the adsorption process were studied: time, adsorbent dose, pH, and Cu²⁺ concentration. The residual concentration of Cu²⁺ ion was determined by spectrophotometer at a fixed wavelength of 470 nm. More details were given in the Supplementary Information.

The amount of adsorbed metal ion (C_a, mg/L) was calculated as follows [13]:

$$C_a = C_0 - C_e \text{ (mg/L)} \quad (1)$$

Where C₀ and C_e are the initial and residual concentrations of metal ions.

The percentage recovery factor (H %) was calculated as follows:

$$H = \frac{C_a}{C_0} \times 100 \text{ (\%)} \quad (2)$$

where C_a and C₀ are the adsorbed and initial concentration of metal ions.

The equilibrium adsorption capacity of SiO₂ NPs towards Cu²⁺ ions was determined according to the equation:

$$q_e = \frac{V_0(C_0 - C_e)}{m} \quad (3)$$

where q_e is the equilibrium adsorption capacity (mg/g), C₀ and C_e are the initial and residual concentrations (mg/L) of Cu²⁺, respectively, V₀ is the initial volume

of Cu²⁺ solution (L), and m is the weight of adsorbent (g).

Determination of equilibrium time

The adsorption equilibrium time was determined by mixing 0.3 g of the adsorbent SiO₂ NPs with 100 mg/L Cu²⁺ ion solution at pH 6, followed by stirring at room temperature for various duration between 0-60 minutes.

Effect of adsorbed dose

To study the effect of SiO₂ NPs dosage on their adsorption capacity, various amounts of SiO₂ NPs between 0.1-0.5 g were added to 100 mL of 40 mg/L Cu²⁺ ion solutions at pH 6, followed by stirring at room temperature for 30 minutes.

Effect of pH

At room temperature, 0.3 g of SiO₂ NPs adsorbent material was added to 100 mL of Cu²⁺ 40 mg/L solution with varying pH values between 1 and 10, followed by 30-minute agitation. pH adjustment was done by adding HCl 0.1 M or NH₃ 0.1M.

Adsorption isotherm

The adsorption isotherms of Cu²⁺ ion were investigated by mixing 0.3 g of SiO₂ NPs adsorbent material with 100 mL of Cu²⁺ solution of different initial concentrations 20-100 mg/ at pH about 6 under room temperature with agitation for 30 min.

The adsorption isotherm of Cu²⁺ ions could be described by the Langmuir and the Freundlich adsorption model.

The Langmuir equation is [9]:

$$\frac{1}{q_e} = \frac{1}{q_{\max} K_L C_e} + \frac{1}{q_{\max}} \quad (4)$$

where q_e and q_{max} are the equilibrium and maximum adsorption capacity of adsorbent (mg/g), respectively; C_e represents the

equilibrium Cu^{2+} concentration in solution (mg/L), and K_L is the Langmuir adsorption constant (L/mg).

The Freundlich equation is [9]:

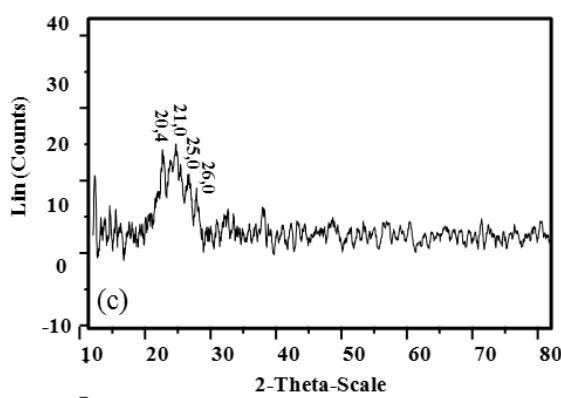
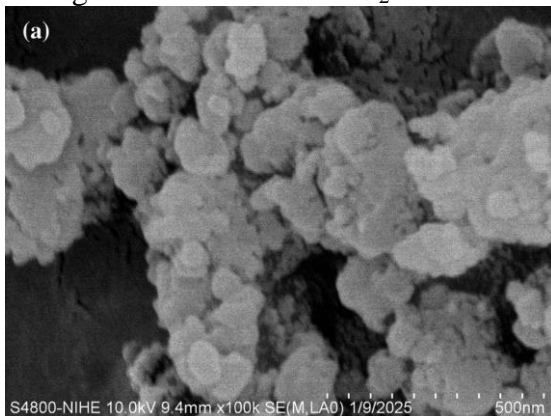
$$\lg q_e = \lg K_F + \frac{1}{n_F} \lg C_e \quad (5)$$

where $n = 1/n_F$ is the slope of Freundlich isotherm, and K_L is the Freundlich adsorption constant.

3. RESULTS AND DISCUSSIONS

Characterization of SiO_2 NPs

Figure 1a and b showed the scanning electron microscopy (SEM) image and energy dispersive X-Ray (EDX) spectra of the SiO_2 NPs sample. SEM images showed spherical particles of SiO_2 NPs with a broad distribution size. The average size of the SiO_2 NPs was



approximately 100 nm in diameter. Moreover, many particles aggregated to create porous structures. The composition of these nanoparticles (Figure 1b) was analyzed by energy-dispersive X-ray spectroscopy (EDX). The results indicated that these SiO_2 nanoparticles were composed of C (27 % from the carbon on the substrate or residual), Si (28.78 % from SiO_2 NPs), and O (57.92 % from SiO_2). Furthermore, no metal element was detected in the EDX result, showing that the SiO_2 NPs product from our synthesis process was high quality.

Next, the diffraction pattern of the SiO_2 NPs in Figure 1c showed a widened peak at 20 about 20-25°. XRD measurement indicated that the as-synthesized SiO_2 NPs were primarily amorphous [14].

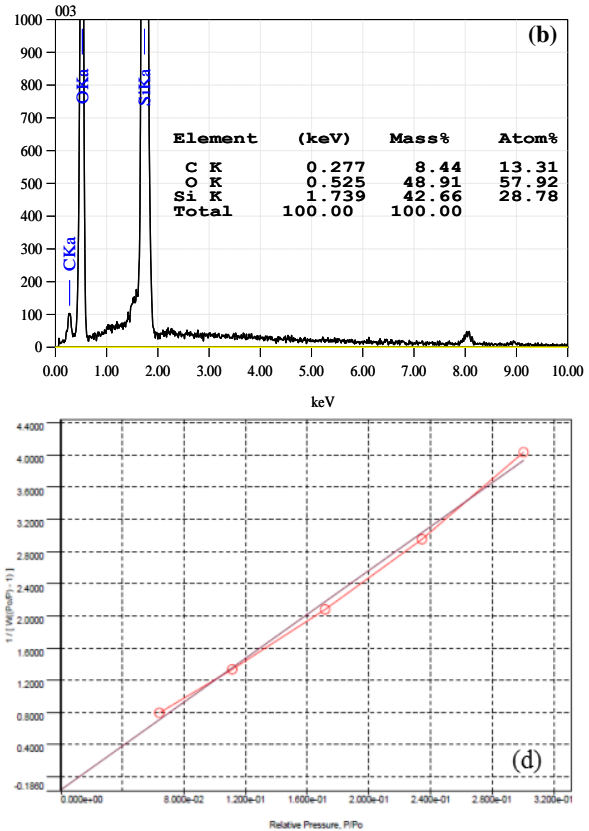


Figure 1. (a) SEM image of SiO_2 NPs. (b) EDX spectrum of SiO_2 NPs. (c) XRD pattern of SiO_2 NPs. (d) BET result of SiO_2 NPs

The specific surface area of the SiO_2 NPs sample (Figure 1d) was determined by BET (Brunauer–Emmett–Teller) measurement [14]. The specific surface area of SiO_2 NPs was approximately $250 \text{ m}^2/\text{g}$. This porosity was an essential feature of SiO_2 NPs synthesized from RHA for their potential application as adsorbent materials.

Determination of equilibrium time

Our data (Figure 2 and Table S1) indicate that the Cu^{2+} adsorption depended on the mixing time with adsorbent SiO_2 NPs. Figure 4 showed that adsorption occurred rapidly in the first 20 minutes. Then, the adsorption rate slowed and almost reached equilibrium at 30 minutes. As a result, 30 minutes was considered the optimized time for Cu^{2+} ion adsorption into SiO_2 NPs.

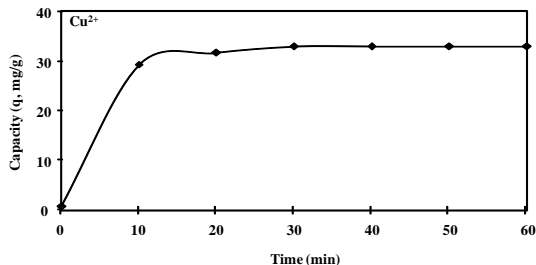


Figure 2. Effect of time on the adsorption process of Cu^{2+} ion.

Effect of adsorbed dose

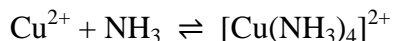
The results in Table S2 showed that the adsorption capacity increased when reducing the amount of SiO_2 NPs and q_e reaching the maximum value (35.9 mg/g for Cu^{2+}) corresponding to the amount of SiO_2 NPs 0.1 g . Due to the small amount of SiO_2 NP content, the SiO_2 was well dispersed in aqueous solution. Thus, Cu^{2+} ion dispersed rapidly to the SiO_2 NPs surface, leading to stronger and faster adsorption capacity to reach equilibrium. However, the percentage recovery factor ($H \text{ } \%$) was 89.86% for Cu^{2+} ,

corresponding to the amount of SiO_2 NPs 0.1 g . In comparison, the maximum percentage recovery factor ($H\%$) was 99.70% for Cu^{2+} , corresponding to the amount of SiO_2 NPs 0.3 g . Therefore, we choose 0.3 g of SiO_2 NPs as a suitable condition for subsequent studies.

Effect of pH

When adjusting the pH of the Cu^{2+} solution between 2-10, we observed that the adsorption capacities of SiO_2 NPs towards Cu^{2+} ions increased with the pH rise (Table S3). When pH was less than 4.0, the adsorption capacities for Cu^{2+} were low, while the maximum adsorption capacities for Cu^{2+} were obtained at pH 5-6, reaching 13.28 mg/g . This effect of pH on the adsorption was explained by Zhu *et al.* [9]. Their study explained that when the pH value was below 2, the silica surface was positively charged, resulting in electrostatic repulsion between the adsorbent and metal ion. The lower the pH, resulted in the higher the repulsion, thus decreasing the adsorption capacity. In contrast, when the pH exceeded 2, the silica surface was more negatively charged, leading to electrostatic attraction between SiO_2 NPs and Cu^{2+} . As the solution pH rose further, the H^+ ions would combine with silanol groups on the surface and dissociated, creating more active sites for adsorption and the activity of hydroxyl groups on the surface. These effects led to an increase in the removal percentage and adsorption capacity of heavy metal ions. In our case of Cu^{2+} adsorption, when $\text{pH} < 6$, the decrease of Cu^{2+} dissolving in solution was due to the adsorption activity of the adsorbent. Meanwhile, when $\text{pH} > 6$, the removal of Cu^{2+} was due to adsorption and precipitation, where precipitation was the dominant process. Nevertheless, the pH of metal ion solutions was adjusted to the

desired value by adding HCl 0.1 M or NH₃ 0.1 M. When pH > 8, the increase of dissolving Cu²⁺ in the solution was because of a complex reaction of copper with NH₃ such as:



Therefore, the pH value of Cu²⁺ solution suitable for absorption on SiO₂ NPs was around 5-6.

Adsorption isotherm

After determining the suitable condition for adsorption, e.g., adsorbent dose, mixing time, and pH, the adsorption isotherm of Cu²⁺ ion was studied by testing 0.3 g of SiO₂ NPs adsorbent material with 100 mL of Cu²⁺ solution at different initial concentrations 20-100 mg/L at pH 6 under agitation for 30 minutes at room temperature. The data in Table S4 demonstrated that when the concentration of Cu²⁺ gradually increased, the adsorption capacity elevated, and the adsorption efficiency diminished. Especially when the concentration of Cu²⁺ was higher than 60 mg/L, the percentage recovery factor (H %) was reduced.

Furthermore, we analyzed the Cu²⁺ adsorption process on SiO₂ NPs using the Langmuir and the Freundlich adsorption model [9], as shown in Figure 3. Langmuir adsorption isotherm was based on the assumption that monolayer adsorption occurred on a homogeneous adsorbent surface. Meanwhile, the Freundlich adsorption isotherm assumed that multilayer adsorption occurred in a heterogeneous adsorbent. From Figure 3, our data fit better the Langmuir model than the Freundlich model, suggesting that the studied adsorption process is homogeneous. Based on the Langmuir adsorption model, we calculated that the maximum adsorption capacity for Cu²⁺ of the SiO₂ NPs synthesized from RHA was

76.90 mg/g. Notably, our SiO₂ NPs synthesized from RHA exhibited a higher maximum adsorption capacity than the reported SiO₂ NPs derived from silica fume by microwave synthesis [9], highlighting the potential of both the synthesis method employed in this study and the SiO₂ NPs derived from RHA. Our SiO₂ NPs synthesized from RHA also had an adsorption capacity higher or comparable with the already published data of other sorbents [15].

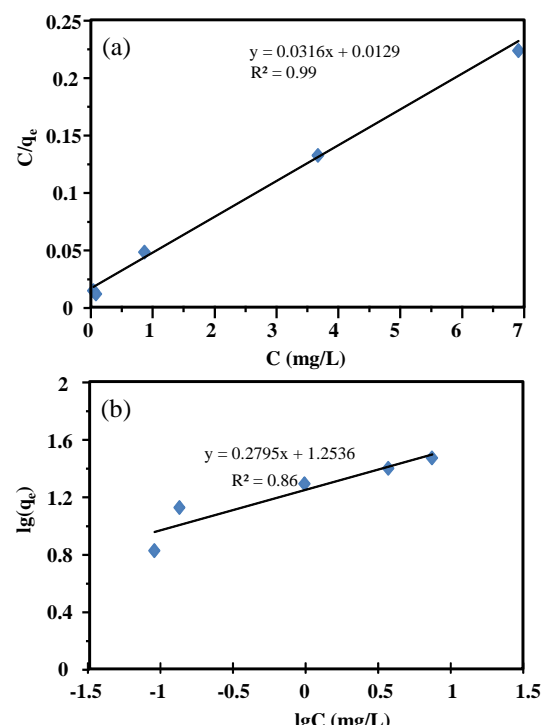


Figure 3. Adsorption isotherm of Cu²⁺ following the model of (a) Langmuir, (b) Freundlich.

Table 1. Fitted adsorption parameters and correlation coefficients for the Langmuir and Freundlich isotherm models

Langmuir			Freundlich		
K _L (L/mg)	q _{max} (mg/g)	R ²	n _F	K _F	R ²
0.41	76.90	0.99	3.58	13.34	0.86

4. CONCLUSIONS

SiO₂ NPs were prepared from rice husk ash using the sol-gel method.

Characterizations of SiO_2 NPs were performed using EDX, XDR, SEM, TEM, and BET methods. The results showed that SiO_2 NPs were mainly in the amorphous phase and had a large specific surface area of about $250 \text{ m}^2/\text{g}$ and particle size of about 100 nm. Moreover, in the optimized conditions, including time, adsorbent dosage, and pH, SiO_2 NPs from RHA could remove Cu^{2+} . The adsorption data of Cu^{2+} had a good fit with the Langmuir isotherm, indicating a homogenous adsorption process. The maximum adsorption capacity for Cu^{2+} was 76.90 mg/g. The enhanced adsorption capacity of the synthesized SiO_2 nanoparticles demonstrated the effectiveness of the proposed synthesis approach. This finding supported the potential application of RHA-derived SiO_2 NPs in heavy metal removal and other adsorption-related processes, with promising implications for cost-effective and scalable implementation.

REFERENCES

- [1]. Ghani A. (2011). Effect of chromium toxicity on growth, chlorophyll and some mineral nutrients of brassica juncea L. *Egyptian Academic Journal of Biological Sciences*, **2** (1), 9-15.
- [2]. Wójtowicz A., Stokłosa A. (2002). Removal of heavy metal ions on smectite ion-exchange column. *Polish Journal of Environmental Studies*, **11** (1), 97-101.
- [3]. Al-Rashdi B. A. M., Johnson D. J., Hilal N. (2013). Removal of heavy metal ions by nano-filtration. *Desalination*, **315**, 2-17.
- [4]. Yun H. C., Prasad R., Guha A. K., Sirkar'a K. K. (1993). Hollow fiber solvent extraction removal of toxic heavy metals from aqueous waste streams. *Industrial and Engineering Chemistry Research*, **32** (6), 1186-1195.
- [5]. Gupta V. K., Ali I., Saleh T. A., Nayak A., Agarwal S. (2012). Chemical treatment technologies for wastewater recycling-an overview. *RSC Advances*, **2**, 6380-6388.
- [6]. Feng Y., Gong J. L., Zeng G. M., Niu Q. Y., Zhang H. Y., Niu C. G., Deng J. H., Yan M. (2010). Adsorption of $\text{Cd}(\text{II})$ and $\text{Zn}(\text{II})$ from aqueous solutions using magnetic hydroxyapatite nanoparticles as adsorbents. *Chemical Engineering Journal*, **162**, 487-494.
- [7]. Albadarin A. B., Mangwandi C., Al-Muhtaseb A. A. H., Walker G. M., Allen S. J., Ahmad M. N. M. (2010). Kinetic and thermodynamics of chromium ions adsorption onto low-cost dolomite adsorbent. *Chemical Engineering Journal*, **179**, 193-202.
- [8]. Dixit D., Biswal V., Singhi V., Goyal R., Kumar D., Ansari A. (2017). Formation of silica gel and gas pollutant adsorption. *International Research Journal of Engineering and Technology*, **4** (8), 2083-2085.
- [9]. Zhu W., Wang J., Wu D., Li X., Luo Y., Han C., Ma W., He S. (2017). Investigating the heavy metal adsorption of mesoporous silica material prepared by microwave synthesis. *Nanoscale Research Letter*, **12** (1), 323.
- [10]. Lê Thị Mai Dung, Đinh Thị Dịu, Nguyễn Thị Hà, Đoàn Thị Hải Yến, Phạm Tiến Đức (2023). Nghiên cứu xử lý Cu^{2+} trong môi trường nước bằng phương pháp hấp phụ sử dụng vật liệu nanosilica vỏ trầu. *Tạp chí phân tích Hóa, Lý và Sinh học*, **29** (2), 112-116.
- [11]. Perdigoto M. L. N., Martins R. C., Rocha N., Quina M. J., Gando-Ferreira L., Patrício R., Durães L. (2012). Application of hydrophobic silica based aerogels and xerogels for removal of toxic organic compounds from aqueous solutions. *Journal of Colloid and Interface Science*, **380** (1), 134-140.

[12].Rahman I. A., Padavettan V. (2012). Synthesis of silica nanoparticles by sol-gel: Size-dependent properties, surface modification, and applications in silica-polymer nanocomposites - A review , *Journal of Nanomaterials*, **2012**, 132424.

[13].Ahmad I., Siddiqui W. A., Ahmad T. (2017). Synthesis, characterization of silica nanoparticles and adsorption removal of Cu^{2+} ions in aqueous solution. *International Journal of Emerging Technology and Advanced Engineering*, **7**, 439-445.

[14].Sankar Sekar, Sanjeev Kumar Sharma, Narinder Kaur, Byoungho Lee, Deuk Young Kim, Sejoon Lee, Hyun Jung (2016). Biogenerated silica nanoparticles synthesized from sticky, red, and brown rice husk ashes by a chemical method, *Ceramics International*, **42** (4), 4875-4885.

[15].Vesna Krstić, Tamara Urošević, Branka Pešovski (2018). A review on adsorbents for treatment of water and wastewaters containing copper ions. *Chemical Engineering Science*, **192**, 273-287.

Supplementary Information

Determination of Cu^{2+} concentration in aqueous solution

The Cu^{2+} solution sample was treated with a nitroso-R reagent to induce complex. Then, we measured the mixture's optical absorbance (Abs) at the maximum absorption of λ_{max} to about 470 nm on UV-DR3900- Hach, USA. Thus, the calibration graph of ion Cu^{2+} solution at λ_{max} to about 470 nm with varying initial ion metals concentration from 0-10 mg/L was obtained in Figure S1.

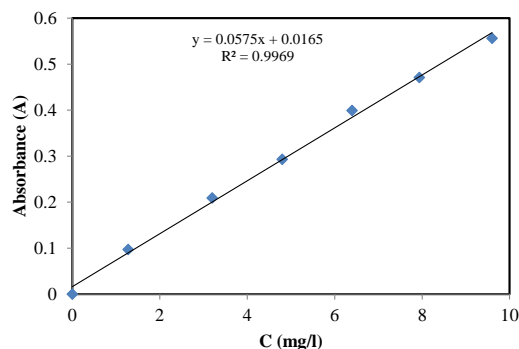


Figure S1: The calibration graph of ion Cu^{2+} solution at λ_{max} to about 470 nm

Table S1. The effect of time on the adsorption capacity of SiO_2 NPs for Cu^{2+} ion

Time (min)	SiO_2 (g)	Volume (L)	C_0 of Cu^{2+} (mg/L)	C_e of Cu^{2+} (mg/L)	Capacity q_t (mg/g)
0	0.3	0.1	100	100	0.00
10	0.3	0.1	100	13.63	28.79
20	0.3	0.1	100	6.65	31.11
30	0.3	0.1	100	3.03	32.32
40	0.3	0.1	100	3.01	32.33
50	0.3	0.1	100	2.94	32.35
60	0.3	0.1	100	2.92	32.36

Table S2. The effect of adsorbent dosage of SiO_2 NPs on the adsorption capacity for Cu^{2+} ion

SiO_2 (g)	0.1	0.2	0.3	0.4	0.5
C_0 (mg/L)	40	40	40	40	40
C_e (mg/L)	4.05	1.44	0.12	0.08	0.07
q_e (mg/g)	35.95	19.28	13.29	9.98	7.99
H (%)	89.86	96.39	99.70	99.80	99.83

Table S3. The effect of Cu^{2+} solutions pH on the adsorption behaviors

pH of Cu^{2+} solution	2	4	6	8	10
C_o (mg/L)	40	40	40	40	40
C_e (mg/L)	3.55	3.95	0.14	0.46	3.79
q_e , (mg/g)	12.15	12.02	13.28	13.18	12.07
H (%)	91.13	90.12	99.64	98.85	90.52

Table S4. The effect of concentration Cu^{2+} solution on the adsorption capacity

C_0 (mg/L)	20	40	60	80	100
C_e (mg/L)	0.08	0.15	0.62	1.54	3.13
q_e (mg/g)	6.64	13.28	19.79	26.15	32.28
H (%)	99.60	99.63	98.97	98.06	96.87